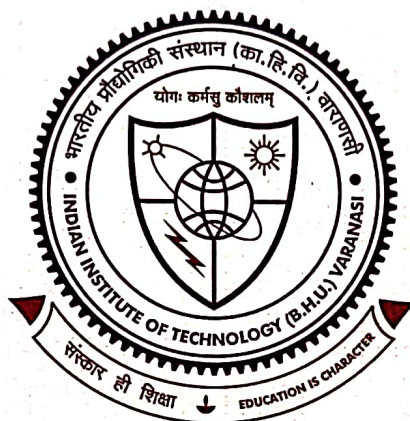


Design, Synthesis, And Biological Evaluation of Mechanism Based Potent AChE and BChE Inhibitors Exhibiting Multifunctional Properties For The Management of Alzheimer's Disease



Thesis submitted in partial fulfillment for the
Award of Degree

Doctor of Philosophy

By

Gauri Shankar

DEPARTMENT OF PHARMACEUTICAL ENGINEERING & TECHNOLOGY
INDIAN INSTITUTE OF TECHNOLOGY
(BANARAS HINDU UNIVERSITY)
VARANASI - 221005
INDIA

Roll No. 19161502

Year 2025



Department of Pharmaceutical Engineering & Technology
Indian Institute of Technology
(Banaras Hindu University)

CERTIFICATE

It is certified that the work contained in the thesis titled "***Design, Synthesis, And Biological Evaluation of Mechanism Based Potent AChE and BChE Inhibitors Exhibiting Multifunctional Properties For The Management of Alzheimer's Disease***" by ***Gauri Shankar*** has been carried out under my supervision and that this work has been not submitted elsewhere for a degree.

It is further certified that the student has fulfilled all the requirements of Course work, Comprehensive, Candidacy, SOTA and Pre-submission seminar.

Gyan Prakash Modi 29/11/25

Dr. Gyan Prakash Modi

Department of Pharmaceutical Engineering & Technology

Indian Institute of Technology (BHU), Varanasi



Department of Pharmaceutical Engineering & Technology
Indian Institute of Technology
(Banaras Hindu University)

DECLARATION BY THE CANDIDATE

I, **Gauri Shankar**, certify that the work embodied in this Ph.D. thesis is my own bonafide work and carried out by me under the supervision of **Dr. Gyan Prakash Modi** from **January, 2020 to July, 2025** at the **Department of Pharmaceutical Engineering & Technology**, Indian Institute of Technology (B.H.U.), Varanasi. The matter embodied in this thesis has not been submitted for the award of any other degree/diploma.

I declare that I have faithfully acknowledged and given credits to the research workers wherever their works have been cited in my work in this thesis. I further declare that I have not willfully copied any other's work, paragraphs, text, data, results, etc., reported in journals, books, magazines, reports, dissertations, thesis, etc., or available at websites and have not included them in this Ph.D. thesis and have not cited as my own work.

Date: 29/04/25
Place: Varanasi

Gauri Shankar
(Gauri Shankar)

CERTIFICATE FROM THE SUPERVISOR

It is certified that the above statement made by the student is correct to the best of my/our knowledge.

Gyan Prakash Modi 29/4/25
(Dr. Gyan Prakash Modi)
Supervisor

K.S. 29/4/25
(Prof. Sairam Krishnamurthy)
Head of the Department
विभागाध्यक्ष / Head

भैषजकीय अभियांत्रिकी एवं प्रौद्योगिकी विभाग /
Department of Pharmaceutical Engineering & Technology
भारतीय प्रौद्योगिकी संस्थान / INDIAN INSTITUTE OF TECHNOLOGY
(बनारस हिन्दू विश्वविद्यालय) / (BANARAS HINDU UNIVERSITY)
वाराणसी-221005 / Varanasi-221005



Department of Pharmaceutical Engineering & Technology
Indian Institute of Technology
(Banaras Hindu University)

COPYRIGHT TRANSFER CERTIFICATE

Title of the Thesis: “Design, Synthesis, And Biological Evaluation of Mechanism Based Potent AChE And BChE Inhibitors Exhibiting Multifunctional Properties For The Management of Alzheimer's Disease”.

Name of the Student: Mr. Gauri Shankar

Copyright Transfer

The undersigned hereby assigns to the Indian Institute of Technology (B.H.U.), Varanasi all rights under copyright that may exist in and for the above thesis submitted for the award of the “*Doctor of Philosophy*”.

Date:

Place:

Gauri Shankar
(Gauri Shankar)

Note: However, the author may reproduce or authorize others to reproduce material extracted verbatim from the thesis or derivative of the thesis for author's personal use provided that the source and the Institute's copyright notice are indicated.

Acknowledgments

I am deeply privileged to express my heartfelt gratitude to Bharat Ratna Pandit Madan Mohan Malviya ji for his visionary efforts in establishing the sacred institution of learning, Banaras Hindu University. His unparalleled dedication has created a place that continues to inspire countless minds.

I would also like to extend my profound gratitude to Dr. Gyan Prakash Modi for his invaluable mentorship, insightful guidance, and unwavering support throughout the early stages of my research and beyond. His steadfast encouragement and unparalleled advice have been instrumental in shaping my academic journey and my personal growth. His exceptional scientific acumen and relentless passion for research have been a constant source of inspiration, enriching my evolution as a student, a budding researcher, and an aspiring scientist. I remain deeply indebted to him for his support, which has impacted my life and career in ways words cannot fully express.

I express my heartfelt gratitude to the esteemed Director, Prof. Amit Patra, and the former Director, Prof. P. K. Jain, of the Indian Institute of Technology (BHU), Varanasi, for their visionary leadership and unwavering support. Their provision of essential resources and access to state-of-the-art instrumental facilities was pivotal in ensuring the seamless execution of my research endeavors.

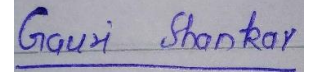
I am profoundly thankful to Prof. S. Hemalatha, Head of the Department of Pharmaceutical Engineering & Technology, IIT (BHU), for his generosity and thoughtful support in granting me access to the requisite infrastructure and resources necessary to complete my research. His kindness and encouragement have been truly inspiring.

My deepest appreciation extends to the members of my Research Progress and Evaluation Committee (RPEC): Dr. Deepak Kumar and Dr. Sanjay Kumar (School of Biochemical Engineering, IIT (BHU)). Their steadfast encouragement, insightful feedback, and unwavering guidance have been instrumental in navigating my research journey toward its successful culmination. Their profound wisdom and support have been invaluable in shaping the direction and quality of my work.

I am also sincerely grateful to the distinguished faculty members of the Department of Pharmaceutical Engineering & Technology, including Prof. B. Mishra, Prof. S.K. Singh, Prof. Sanjay Singh, Prof. S.K. Shrivastava, Dr. S. Krishnamurthy, Dr. (Mrs.) Siva Hemalatha, Dr.

Senthil A. Raja, Dr. A. N. Sahu, Dr. (Mrs.) Ruchi Chawla, Dr. M. S. Muthu, Dr. S. K. Mishra, Dr. S.K. Jain, Dr. A. K. Agrawal, Dr. Vinod Tiwari, Dr. Rajnish, Dr. Deepak Sharma, Dr. Jairam Meena, Dr. Dinesh Kumar, and Dr. Ashok Kumar. Their unwavering cooperation, encouragement, and support are the cornerstone of my academic and research journey. Their collective wisdom and generosity have indelibly impacted my personal and professional growth. I extend my heartfelt gratitude to the dedicated office and technical staff of the Department of Pharmaceutical Engineering & Technology, Indian Institute of Technology (BHU), for their tireless efforts in maintaining an exceptional research environment that has facilitated my work. My sincere appreciation also goes to our esteemed collaborators: Dr. Saroj Kumar and Ms. Sanskriti Rai (AIIMS Delhi), Prof. Prabha Garg and Aritra Banerjee, Mushtaq Ahmad Wani and TanmayKumar Verma (NIPER Mohali), Prof. S. Srikrishna and Mr. Prabhat Kumar (Department of Biochemistry, BHU), and Dr. V.G.M. Naidu and Dr. Samir Kumar Panda. Their invaluable expertise, support, and collaboration have enriched my research journey. I am deeply grateful to all my lab mates, seniors, and super seniors, whose unwavering moral, social, and technical support gave me strength and guidance throughout my research. Their camaraderie and encouragement were a constant source of motivation. I owe a special debt of gratitude to the Science & Engineering Research Board and Indian Council of Medical Research, Government of India, for their financial assistance, which enabled me to sustain my livelihood in Varanasi and pursue my research objectives with focus and determination. My profound thanks also extend to the Central Instrumental Facility (CIF) at IIT (BHU) for providing access to advanced NMR and confocal microscopy facilities, as well as to the Department of Chemistry (BHU) for the HRMS facility. These state-of-the-art resources were invaluable in the successful execution of my research. Last but certainly not least, I wish to convey my heartfelt and sincere gratitude to my family. To my admirable mother and incredible father, whose unwavering love and steadfast support have been the cornerstone of my strength; to my loving wife, whose constant encouragement and understanding have been a source of profound inspiration; to my caring brother and ever-supportive sister, whose kindness and assistance have lightened my burdens their collective faith in me has been instrumental in my journey toward success

I also take immense pride and privilege in extending my deepest thanks to everyone who, directly or indirectly, contributed to the successful completion of my research. Their guidance, encouragement, and support have made this endeavor indelible.

A rectangular box containing a handwritten signature in blue ink that reads "Gauri Shankar".

Gauri Shankar

Date: 24/01/2025

Place: IIT(BHU), Varanasi

List of Figures

Figure 1.1. Diagrammatic representation of ACh synthesis, metabolism, and its mode of action.	6
Figure 1.2. Mechanism of substrate cleavage through AChE.....	7
Figure 1.3. Fenton reaction by which H ₂ O ₂ forms hydroxyl radical in iron-rich environment.	11
Figure 1.4. Schematic representation of the role of iron in AD.	12
Figure 1.5. Diagrammatic representation indicating the role of ROS and metals in AD progression.	13
Figure 1.6. Diagrammatic representation indicating the role of β -secretase in A β aggregation.....	14
Figure 1.7. Schematic view of the active site of AChE.....	18
Figure 1.8. NMDA receptor complex as a therapeutic target in AD.	19
Figure 2.1: Structure of marketed drugs reported as cholinesterase inhibitors.	24
Figure 2.2: Structures of the marketed drug reported as NMDA receptor antagonists.	25
Figure 2.3: Structure of compounds reported in antioxidant therapy of AD.....	26
Figure 2.4: Structure of metal chelators under investigation.	27
Figure 2.5: Binding mechanistic of RIV towards the cholinesterase enzyme	30
Figure 2.6: Structure of lead fluorenyl-based urea derivatives reported by Zahra Rezaei et al.	31
Figure 2.7: Structure of lead pyrazinyl ureas derivatives reported by Park et al.	31
Figure 2.8: Structure of lead propargylamine-modified pyrimidinylthiourea derivatives reported by Xu, Wang, et al.....	32
Figure 2.9: Structure of lead 7-methoxytacrine (7-MEOTA)-amantadine urea derivatives reported by Spilovska et al.....	33
Figure 2.10: Structure of lead benzofuranylthiazole derivatives reported by Kurt, Gazioglu, et al.....	34

Figure 2.11: Structure of lead 1,3-diaryl-urea derivatives reported by Zarghi et al.....	34
Figure 2.12: Design of tryptamine, naringenin and tacrine carbamate hybrids.	36
Figure 2.13: Design and SAR study of cannabidiol-carbamate hybrids.	38
Figure 2.14: Structures and SAR of arylcarbamate-N-acyl hydrazone hybrids.....	39
Figure 2.15: Design and SAR study of ferulic acid-O-carbamoyl derivatives.	40
Figure 2.16: Design and SAR study of N-alkylpiperidine carbamate hybrids.	41
Figure 2.17: Design of chalcone, quinoline, pyridine, and diosgenin-carbamate hybrids.....	42
Figure 2.18: Design of smilagenin, and arctigenin-carbamate hybrids.....	43
Figure 2.19: Design and SAR study of pyraoisoflavone and 4-aminochalcone-RIV hybrids. .	44
Figure 2.20: Design and SAR study of salicylanilide and 4-chlorophenol-based carbamate hybrids.....	45
Figure 2.21: Design of 2-methoxy-phenyl dimethyl-carbamate hybrids.	46
Figure 2.22: Miscellaneous hybrids analogues (67-75).	49
Figure 2.23: Miscellaneous hybrids analogues (50-58).	50
Figure 3.1: The rationale of 1 st series of design molecules.	56
Figure 3.2: The rationale of 2 nd series of designed molecules.	59
Figure 3.3: Overview of the designed study.....	61
Figure 4.1: Design approach towards synthesizing diarylurea-hydroxyamidine derivatives as potential anti-AD agents.....	68
Figure 4.2: Lineweaver-Burk plots illustrate <i>h</i> AChE and <i>eq</i> BChE hydrolytic activity over a range of substrate concentrations and in the presence of different concentrations of inhibitor 3q (A and B), and 6e (C and D).	77

Figure 4.3: 3D docking poses of AChE with (A) 3q (B) 6e , and 2D interaction of AChE with (A1) 3q (B1) 6e where green-, red- and violet-colored arrows represent the π - π stacking, π - cation interactions and hydrogen bonds, respectively.....	81
Figure 4.4: 3D docking poses of BChE with (A) 3q (B) 6e and 2D interaction diagram of BChE with (A1) 3q (B1) 6e where green-, red- and violet-colored arrows represent the π - π stacking, π -cation interactions, and hydrogen bonds, respectively.	82
Figure 4.5: AChE-ligand interaction diagrams for the 300 ns simulation with (A) DPZ (B) RIV (C) 3q (D) 6e showing interaction time percentages with the residues.	84
Figure 4.6: BChE-ligand interaction diagrams for the 300 ns simulation with (A) Tacrine (B) RIV (C) 3q (D) 6e showing interaction time percentages with the residues.	85
Figure 4.7: The graph represents the percent radical scavenging activity of 3q , 6a , 6b , 6e , Quercetin and RIV. Each assay was performed in triplicate. The values are presented as the mean \pm SD.....	86
Figure 4.8: The study investigated the inhibitory effects of 3q and 6e on the self-induced aggregation of A β ₁₋₄₂	88
Figure 4.9: Surface representation of (A) 3q and (B) 6e docked into the pocket of A β ₁₋₄₂ protofibrils and 2D interaction diagram of (A1) 3q and (B1) 6e of the docked complexes.	90
Figure 4.10: RMSD of the backbone atoms of protofibril (black), protofibril- 3q complex (blue), and protofibril- 6e (green) complex for the last 50 ns of the molecular dynamic simulation.....	91
Figure 4.11: Inhibition of self-induced Tau protein aggregation in the presence of 3q and 6e . 92	
Figure 4.12: Graphical representation of 3q , 6e and standard reference curve of nitrite concentration measurement at 520 nm.....	94
Figure 4.13: The impact of 3q and 6e on cellular viability.....	95
Figure 4.14: Effect of 3q and 6e against H ₂ O ₂ mediated cell death.....	96
Figure 4.15: The effect of 3q and 6e on apoptosis.....	98

Figure 4.16: Compounds **3q** and **6e** exert microglial cell proliferation and attenuate the ROS and MMP damage caused by LPS and ATP. 100

Figure 4.17: Compounds **3q** and **6e** inhibit microglial activation and subside the NF- κ B and NLRP3 inflammasome activation as evidenced by Immunocytochemistry (ICC) staining of HMC-3 cells for NLRP3, NF- κ B, Vimentin and Phalloidin Red..... 102

Figure 4.18: Compounds **3q** and **6e** inhibited microglia activation and NLRP3 inflammasome activation. 104

Figure 4.19: Represents the examination of **3q**, **6e**, and RIV drugs on OregonR+ and AD flies.....107

Figure 4.20: Mitochondrial superoxide (ROS) level measurement in Oregon+ and A β ₁₋₄₂ expressing eye imaginal discs of Drosophila.110

Figure 4.21: Measurement of total cellular ROS level in OregonR+ and A β ₁₋₄₂ expressing eye imaginal discs of Drosophila.....111

Figure 4.22: The graph represents the average daily body weight of each group of mice over a 14-day period of drug administration with a dosage of **3q** and **6e** at 2000 mg/kg..... 113

Figure 4.23: The study examined the impact of **3q** and **6e** on memory deficits induced by scopolamine in the Y-maze test.114

Figure 4.24: The ex-vivo analysis of mice hippocampus with AChE, BChE, SOD Catalase, and MDA levels by the scopolamine-treated group with various treatment groups of **3q** and **6e**, respectively.....116

Figure 4.25: Performance of mice in Morris water maze.118

Figure 4.26: A. Graph represents latency of mice in control, disease control, standard control, **3q** and **6e** groups in Passive avoidance; B. Graph represents relative gene expression/ GAPDH of mice in different treatment groups: BDNF, TRKB, CREB1, PSD 95, C-FOS, PKA, NR4a2, GAP 43..... 121

Figure 4.27: Design approach towards synthesizing tryptamine derivatives and role of RIV fragment that can also serve as a template to fine-tune physicochemical properties of the parent compound.	124
Figure 4.28: 2D and 3D docking interactions of 15d and 15e against AChE and BChE protein.....	132
Figure 4.29: 2D interaction diagrams showing the binding of RIV, 15d and 15e with AChE and BChE.....	134
Figure 4.30: 3D interaction diagrams showing the binding of RIV, 15d and 15e with AChE and BChE.....	135
Figure 4.31: Molecular dynamics trajectory analysis of compounds 15d and 15e with AChE and BChE complex.....	137
Figure 4.32: Graphical representation of % Radical scavenging activity of lead compound 15d , 15e , and marketed drug RIV.	138
Figure 4.33: The impact of 15d and 15e on cellular viability.	140
Figure 4.34: Cells were pre-incubated with 15d (A) and 15e (B) at 1, 2.5, 5, 7,10, 15, or 20 μ M for 24 h and then further incubated with 600 μ M H ₂ O ₂ for another 24 h.	141
Figure 4.35: The effect of neuroprotective compounds 15d and 15e on apoptosis	143
Figure 4.36: UV-visible spectroscopic scanning of a solution containing 300 μ M of 15d and 15e alone in methanol or combined with 300 μ M of FeCl ₃ and CuSO ₄ at pH 7.4, covering the 300-550 nm range.....	144
Figure 4.37: Inhibition of self-induced A β ₁₋₄₂ aggregation in the presence of 15d or 15e	146
Figure 4.38: Morphological evaluation of A β ₁₋₄₂ by TEM imaging in the absence and presence of compounds 15d or 15e	147
Figure 4.39: (a) 2D interaction diagram of 15d	148
Figure 4.40. (a) The radius of Gyration (b) SASA and (c) Mmgbsa calculated over the trajectories.	149

Figure 4.41: Free-energy contribution of critical residues from different chains (highlighted in different colors) of protofibril to (a) 15d and (b) 15e .	150
Figure 4.42: Represents the examination of 15d , 15e , and RIV drugs on OregonR+ and AD flies.	152
Figure 4.43: Mitochondrial superoxide (ROS) level measurement in Oregon+ and A β 42 expressing eye imaginal discs of Drosophila.	153
Figure 4.44: Measurement of total cellular ROS level in OregonR+ and A β 42 expressing eye imaginal discs of Drosophila.	155
Figure 4.45: The graph represents the average daily body weight of each group of mice over 14 days of drug administration with a dosage of 15d and 15e at 175 mg/kg.	156
Figure 4.46: Performance of mice in Morris water maze.	158
Figure 4.47: Effect of RIV, 15d and 15e on various neurochemical parameters such as AChE, BChE, SOD, CAT and MDA.	159
Figure 4.48: RT-PCR analysis of memory markers.	161
Figure A1: ¹ H NMR spectra of (Z)-3-(3-(3-fluorophenyl)ureido)-N'-hydroxybenzimidamide (3q).	235
Figure A2: ¹³ C NMR spectra of (Z)-3-(3-(3-fluorophenyl)ureido)-N'-hydroxybenzimidamide (3q).	236
Figure A3: HRMS spectra of (Z)-3-(3-(3-fluorophenyl)ureido)-N'-hydroxybenzimidamide (3q).	237
Figure A4: ¹ H NMR spectra of (Z)-N'-hydroxy-3-(3-(2-(5-methoxy-1H-indol-3-yl)ethyl)ureido)benzimidamide (6e).	238
Figure A5: ¹³ C NMR spectra of (Z)-N'-hydroxy-3-(3-(2-(5-methoxy-1H-indol-3-yl)ethyl)ureido)benzimidamide (6e).	239
Figure A6: HRMS spectra of (Z)-N'-hydroxy-3-(3-(2-(5-methoxy-1H-indol-3-yl)ethyl)ureido)benzimidamide (6e).	240

Figure A7: ^1H spectra of (S)-3-(1-(dimethylamino)ethyl)phenyl (2-(5-hydroxy-1H-indol-3-yl)ethyl)carbamate (15d).....	241
Figure A8: ^{13}C spectra of (S)-3-(1-(dimethylamino)ethyl)phenyl (2-(5-hydroxy-1H-indol-3-yl)ethyl)carbamate (15d).....	242
Figure A9: HRMS spectra of (S)-3-(1-(dimethylamino)ethyl)phenyl (2-(5-hydroxy-1H-indol-3-yl)ethyl)carbamate (15d)	243
Figure A10: HPLC chromatogram of (S)-3-(1-(dimethylamino)ethyl)phenyl (2-(5-hydroxy-1H-indol-3-yl)ethyl)carbamate (15d).....	244
Figure A11: ^1H spectra of (S)-3-(1-(dimethylamino)ethyl)phenyl (2-(5-chloro-1H-indol-3-yl)ethyl)carbamate (15e)	245
Figure A12: ^{13}C spectra of (S)-3-(1-(dimethylamino)ethyl)phenyl (2-(5-chloro-1H-indol-3-yl)ethyl)carbamate (15e)	246
Figure A13: HRMS spectra of (S)-3-(1-(dimethylamino)ethyl)phenyl (2-(5-chloro-1H-indol-3-yl)ethyl)carbamate (15e)	247
Figure A14: HPLC chromatogram of (S)-3-(1-(dimethylamino)ethyl)phenyl (2-(5-hydroxy-1H-indol-3-yl)ethyl)carbamate (15e)	248

List of Tables

Table 1. Cholinesterase inhibitory activities of the target compounds.	74
Table 2. Cholinesterase inhibitory activities of the target compounds.	75
Table 3. Displacement of Propidium Iodide from the PAS of <i>hAChE</i> by 3q , 6e , DPZ, and RIV.	78
Table 4. Docking score and interactions of the ligands with AChE	79
Table 5. Docking score and interactions of the ligands with BChE	81
Table 6. Antioxidant activity (DPPH assay) of 3q , 6a , 6b , 6e and RIV.....	87
Table 7. Docking score and interactions of the ligands with amyloid beta fibrils	89
Table 8. The permeability (<i>Pe</i>) of 3q , 6e , testosterone, and norfloxacin was determined in the PAMPA assay and was expressed in $Pe = 10^{-6} \text{ cm s}^{-1}$	112
Table 9. AChE and BChE inhibition studies of the synthesized compounds	127
Table 10. Kinetic Values for Carbamoylation on <i>hAChE</i> and <i>eqBChE</i> of lead compound 15e	129
Table 11. Displacement of Propidium Iodide from the PAS of <i>hAChE</i> by 15d , 15e , and RIV..	130
Table 12. Important interactions of compound 15d and 15e , along with the reference standard RIV, with AChE protein (PDB ID: 4EY7).....	130
Table 13. Important interactions of compound 15d and 15e along with the reference standard RIV, with BChE protein (PDB ID: 4BDS).	133
Table 14. Antioxidant activity (DPPH assay) of 14e , 14c , 15d , 15e , ascorbic acid and RIV.	138
Table 15. The permeability (<i>Pe</i>) of 15d , 15e , Testosterone, and Norfloxacin was determined in the PAMPA assay and was expressed in $Pe = 10^{-6} \text{ cm s}^{-1}$	145
Table 16. Physical properties and ADMET prediction of the compounds.....	162
Table 17. HRMS table with their chemical formula and ppm value of all synthesized compounds.	188
Table 18. Comparison of the pharmacological profiles of the lead compounds from both series.	217

List of Schemes

Scheme 1. Synthesis of diphenylurea-amidine derivatives 3a-3w	69
Scheme 2. Synthetic route for compounds 6a-6e	69
Scheme 3. Synthesis of diarylurea-hydroxyamidine derivatives 9a-9e	70
Scheme 4. Synthetic route of compounds 11a-11b	70
Scheme 5. Synthetic route of compounds 12a-14e	125
Scheme 6. Synthetic route of compounds 15a-15e	125
Scheme 7. Synthetic route of compound 16e	126

List of Abbreviations

Abbreviations	Full forms
AD	Alzheimer's disease
ACh	Acetylcholine
<i>h</i> ACh	Human acetylcholine
MW	Molecular weight
MTT	3- (4,5-dimethylthiazol-2-yl)-2,5-diphenyltetrazolium
PAS	Peripheral anionic site
ROS	Reactive oxygen species
TMS	Tetramethylsilane
BChE	Butyrylcholinesterase
BBB	Blood-Brain Barrier
CAS	Catalytic active site
CDCl ₃	Deuterated chloroform
DMSO- <i>d</i> ₆	Deuterated dimethyl sulfoxide- <i>d</i> ₆
DPZ	Donepezil
DTNB	5,5'-dithiobis-2-nitrobenzoic acid
DPPH	2,2-diphenyl-1-picrylhydrazyl
RIV	Rivastigmine
FA	Ferulic acid
MABs	Monoclonal antibodies
JNK	Janus kinase
HRMS	High-resolution mass spectrometry
HOBt	<i>N</i> -hydroxybenzotriazole
IC ₅₀	The inhibitory concentration required to kill 50% of the population
IL-6	Interleukin-6
IL-β	Interleukin-beta
MMP	Mitochondrial membrane potential
TLR4	Toll-like receptor 4-Nucleotide-binding domain, leucine-rich containing
NLRP3	family, pyrin domain-containing-3
CAT	Catalase
MDA	Malondialdehyde
SOD	Superoxide dismutase

List of Symbols

Symbols	Meaning
α	Alpha
β	Beta
δ	Delta
$^{\circ}\text{C}$	Degree Celsius
\AA	Angstrom
mg	Milligram
μg	Micro gram
μM	Micromole
mmol	Millimole
ml	Millilitre
μL	Microliter
h	Hour
s	Singlet
nm	Nanometer
μm	Micrometer
mm	Millimeter
cm	Centimeter
ppm	Parts per million
rpm	Revolutions per minute
Kcal	Kilocalories
Hz	Hertz
MHz	Megahertz
J	Coupling constant
d	Doublet
t	Triplet
q	Quartet
m	Multiplet
dd	Doublet of doublet
m/z	Mass-to-charge ratio
%	Percent
pH	Potential of hydrogen
\leq	Less than or equal
$<$	Less than
$>$	More than
\pm	Plus or minus

Preface

Alzheimer's Disease (AD) is an age-related neurodegenerative disorder that accounts for over 80% of dementia cases in older adults worldwide. It is characterized by a low level of acetylcholine (ACh), an increase in oxidative stress, accumulation of metals, deposition of amyloid-beta ($A\beta$) plaques, and neurofibrillary tangles, leading to the progressive loss of memory and cognitive functions. Despite decades of research on the etiology of the disease and substantial efforts by the pharmaceutical industry to develop effective therapies, no treatment has been found to cure AD or significantly inhibit its progression. Currently, four drugs- donepezil (DPZ), galantamine, rivastigmine (RIV) (acting on the cholinergic pathway), and memantine (acting on the NMDA receptor) are approved by the USFDA. Aducanumab and Lecanemab are monoclonal antibodies (MABs) recently approved for treating AD. These drugs target amyloid-beta ($A\beta$) plaques, which are believed to play a central role in the pathophysiology of AD. As we know, AD is a multifactorial disease; therefore, targeting single drugs is insufficient for comprehensive treatment. Although combination therapies offer dosing flexibility, they pose considerable challenges, such as the risk of drug-drug interactions, complicated treatment protocols, and lower patient compliance. The development of multiple drugs substantially increases research and development costs. In the case of AD therapies, which encompass preclinical studies and clinical trials, these costs frequently surpass \$2 billion, primarily due to the high attrition rates associated with drug development. In contrast, multifunctional ligands offer a more efficient therapeutic strategy by targeting multiple pathological pathways simultaneously, reducing the need for multiple agents. This approach not only simplifies clinical trial design and regulatory approval processes but also potentially lowers overall development costs, providing a more holistic solution to the multifactorial nature of AD.

Rivastigmine (RIV), a second-generation pseudo-irreversible cholinesterase inhibitor, is a widely used therapeutic agent for AD. However, several limitations restrict its efficacy as a comprehensive treatment. RIV shows selective inhibition of butyrylcholinesterase (BChE; $IC_{50} = 91 \pm 0.40$ nM) while only moderately inhibiting acetylcholinesterase (AChE; $IC_{50} = 6630 \pm 0.76$ nM), making it less effective in the earlier stages of AD where AChE activity predominates. Additionally, RIV provides symptomatic relief without targeting the pathological hallmarks of AD, such as oxidative stress, amyloid beta ($A\beta$), and tau protein aggregation, inflammation, and neurodegeneration. Its covalent mechanism of action through carbamylation of the enzyme's active site serine residue further limits its safety profile by causing pseudo-irreversible inhibition and potential off-target effects. To address these drawbacks, we designed two series of multifunctional molecules to enhance therapeutic efficacy.

The first series of molecules focused on improving RIV's limitations by replacing its amine group with aromatic and heterocyclic moieties to enhance interactions with AChE and BChE while modulating $A\beta$ and tau aggregation. The carbamate moiety of RIV was replaced with amidoxime to enhance antioxidant properties and achieve a better balance between hydrophobicity and hydrophilicity. This series showed significant improvement in AChE inhibition, antioxidant properties, and modulation of $A\beta$ and tau aggregation, but BChE inhibition remained suboptimal compared to RIV. In the second series, insights from the literature on carbamate-based selective BChE inhibitors were utilized to design potent inhibitors with additional therapeutic benefits. Substituted tryptamine fragments replaced the N-ethyl-N-methylamine group of RIV to improve multifunctional activity, including inhibition of AChE and BChE, antioxidant effects, and modulation of $A\beta$ aggregation. Chirality was optimized by synthesizing the molecules' racemic and enantiomeric versions, with S-configured analogs

exhibiting superior potency. Compounds such as **15e** and **16e** demonstrated enhanced inhibitory activity and antioxidant and neuroprotective properties, offering a disease-modifying therapeutic approach. These rationally designed molecules aim to overcome the limitations of RIV and provide a comprehensive strategy to target multiple pathological aspects of AD.

The present study is divided into six chapters:

Chapter 1: This chapter overviews AD, including its pathophysiology and the current treatments.

Chapter 2: This chapter comprehensively reviews the literature on the relevant research on carbamate and urea hybrids reported in the last two decades for managing AD.

Chapter 3: This chapter outlines the research work's hypothesis, rationale, and detailed plan related to our proposed work.

Chapter 4: This chapter discusses the rationale for synthesizing and evaluating novel diphenylurea-amidine and carbamate-based tryptamine derivatives. The designed molecules were synthesized and subjected to *in-vitro* enzyme inhibition studies. The potent molecules identified from these studies were further investigated for enzyme kinetics, antioxidant activity, metal chelation, A β modulation, and neuroprotection. Lead compounds were then selected for *in-vivo* studies in AD animal models to evaluate their effects on working memory and learning.

Chapter 5: This chapter details the general synthetic procedures used for the targeted compounds and their subsequent biological evaluation.

Chapter 6: This chapter provides the final summary and conclusions drawn from the research.